J Appl Phycol (2016) 28:2195–2203
DOI 10.1007/s10811-015-0763-6

Improving mass transfer in an inclined tubular photobioreactor

Roger W. Babcock Jr.[1] · **Anke Wellbrock**[1] · **Peter Slenders**[2] · **JoAnn C. Radway**[3]

Received: 25 August 2015 / Revised and accepted: 18 November 2015 / Published online: 3 December 2015

Abstract The mass transfer and hydrodynamics of two outdoor tubular photobioreactor designs were compared, a Tredici-design near-horizontal tubular photobioreactor (NHTR) and an enhanced version of this reactor (ENHTR), for the purpose of improving algal growth via improved hydrodynamics. The enhancements included addition of vertical bubble columns at the sparger end and a larger degasser with a diffuser. Gas-liquid mass transfer and other performance measures were assessed for a range of gas sparging rates. The ENHTR modifications proved to be very successful, increasing oxygen stripping and carbon dioxide dissolution by 120–220 % and 0–50 %, respectively. There was an increase in axial mixing and a fourfold decrease in total mixing time. Experiments were conducted to determine that approximately 50 % of the mass transfer occurred in the vertical bubble columns, while 85–90 % of the mass transfer in the near-horizontal tubes occurred in the lower half of the tubes. These improvements can lead to increased algae productivity depending upon culture-specific parameters. The theoretical maximum productivity of a hypothetical algal culture would be 1.6 g m^{-2} h^{-1} in the NHTR, and we have previously achieved a maximum of 1.5 g m^{-2} h^{-1} growing *Arthrospira* at densities up to 7.5 g L^{-1} in this reactor. Due to enhanced mass transfer in the ENHTR, the predicted maximum productivity should increase to 4.75 g m^{-2} h^{-1}. The potential for further improvements in productivity due to various additional enhancements is described.

Keywords Photobioreactor · Airlift reactor · Microalgae · Mass transfer · Hydrodynamics

Nomenclature

C	dissolved oxygen concentration at time t (mg L^{-1})
C_∞^*	dissolved oxygen saturation concentration at $t=\infty$ (mg L^{-1})
C_o	dissolved oxygen concentration at $t=0$ (mg L^{-1})
ID	axial dispersion coefficient (m^2 s^{-1})
K_La	gas-liquid mass transfer coefficient (h^{-1})
$K_La_O^{20}$	gas-liquid mass transfer O_2 coefficient at 20 °C (h^{-1})
$K_La_C^{20}$	gas-liquid mass transfer CO_2 coefficient at 20 °C (h^{-1})
N	number of CSTRs in series (−)
N_O^{20}	standard deoxygenation rate at 20 °C (mg min^{-1})
N_C^{20}	standard carbonation rate at 20 °C (mg min^{-1})
Re	Reynolds number (−)
v_l	liquid lineal velocity (m s^{-1})
V_{water}	liquid operating volume (L)

Introduction

Microalgal cultivation is used for the commercial production of human food supplements, beta-carotene, waste treatment, aquaculture, and feed in large open systems—lakes or raceways with paddle wheels (Del Campo et al. 2007; Kang et al. 2015; Béchet et al. 2015). While there are potentially many other high value products produced by different microalgae, the cultivation of microalgae in open systems is problematic

✉ Roger W. Babcock, Jr.
rbabcock@hawaii.edu

[1] Civil Engineering Department, University of Hawaii, Honolulu, HI 96822, USA

[2] FEI Company, Trondheim N-7041, Norway

[3] Marine Sciences Center, Stony Brook University, Stony Brook, NY 11794, USA

due to the inability to control contaminants such as bacteria and protozoa that interfere with microalgal growth and reduce purity of final products. Closed system airlift photobioreactors (tubes or plates) can effectively enhance the ability of microalgae to carry out photosynthesis (shorter light paths, better mixing), control gas exchange, and minimize impurities, and many such designs have been created and evaluated (García Malea et al. 2006; Wang et al. 2015). One type of closed photobioreactor is the Tredici near-horizontal tubular reactor (NHTR) (Chini Zittelli et al. 1999).

A photobioreactor is a gas-liquid two-phase system with CO_2 being injected directly into the reactor (via the sparging air), providing inorganic carbon and controlling the pH of the system. The rate of CO_2 introduction into the system controls the rate of photosynthesis and oxygen production. Dissolved oxygen (DO) at high levels of supersaturation is toxic to microalgae (450 % or higher for *Arthrospira*), and therefore, oxygen stripping is required (Vonshak 1997). Maximizing mass transfer of oxygen and CO_2 is a key to controlling oxygen inhibition and maximizing microalgae growth. The oxygen stripping rate is limited by the overall mass transfer coefficient (K_La) and by the saturated dissolved oxygen concentration (from Henry's law), but CO_2 dissolution is essentially unlimited because any amount (up to 100 %) of pure CO_2 can be introduced with the sparging air to give any desired saturation dissolved CO_2 concentration. Hydrodynamic parameters such as superficial gas velocity, bubble volume/velocity/shape, gas holdup, liquid velocity, axial dispersion, and residence time may also affect microalgal productivity and may differ depending upon photobioreactor design. The hydrodynamics and mass transfer of the Tredici NHTR were studied extensively (Babcock et al. 2002) and then modifications were made resulting in an enhanced NHTR (ENHTR). Here, we compare the ENHTR to the original Tredici NHTR design in terms of mass transfer, hydrodynamics, and theoretical productivity.

Materials and methods

Photobioreactor

Hydrodynamics and mass transfer experiments were conducted using two NHTRs located in Honolulu, Hawaii. The Tredici NHTR outdoor photobioreactor has been described in previous studies (Chini Zittelli et al. 1999; Babcock et al. 2002). The NHTR design consists of eight 19.60 m fluoropolymer tubes, 4 cm in diameter, on a 4-degree incline. On the lower end of each tube, a 60-cm segment has a steeper incline (16 degrees). The tubes are connected in parallel to a PVC sparging manifold at the lower end (5.1 cm inner diameter) and a Plexiglas degassing manifold at the upper end (22.8 cm inner diameter, operated less than half full at 11.6-L volume). The total reactor operating volume is 220 L. Operation has the six center tubes (risers) sparged with air (spiked with pure CO_2) for mixing, CO_2 dissolution, and oxygen stripping. As the air is introduced, it coalesces into large bubbles providing airlift and internal gas transfer (CO_2 from the bubbles into the liquid and O_2 from the liquid into the bubbles). The bubbles and liquid flow up through the six riser tubes to the degasser unit and then liquid descends via the two outer un-sparged tubes (downcomers) for flow recirculation. The steeper 60-cm segment ensures rapid bubble coalescence in the riser tubes and minimizes the chance of flow reversal by increasing the localized bubble velocity. During algae production operations, the CO_2 injection rate into the sparger is regulated via a pH controller.

The ENHTR maintains the design of eight 19.60 m tubes at a 4-degree incline leading to the degasser and the 0.60 m section at 16-degree incline at the lower end. A modified sparger manifold was fabricated from Plexiglas (increased from 5.1 to 7.6 cm diameter). Acrylic vertical bubble columns (VBCs) 100 cm long, 3.8 cm inside diameter, were added between the sparger manifold and the end of the 8-parallel inclined tubes. To ensure even airflow into each of the six aerated VBCs, each contained a fine-bubble diffuser stone at 11.5 cm above the center of the sparger manifold with its own flowmeter. The degasser located at the upper end of the reactor was modified into a wedge-shaped box (26 L liquid volume) containing a sparger tube to enhance degassing. These modifications increased the ENHTR operating volume to 252 L. During mass transfer experiments, the six center VBCs were sparged with air and the introduced bubbles remained small (approximately 4 to 8 mm diameter) until they reached the connection with the inclined tubes, after which, they rapidly coalesced just as in the NHTR. A schematic diagram for the ENHTR is shown in Fig. 1.

A cooling system was utilized for both reactor designs consisting of a 30 sprinkler-head system spraying tap water on top of the tubes to facilitate evaporative cooling. The temperature was regulated by a datalogger that controlled the cooling water supply valve, using readings (2-minute interval) from thermocouples in the reactor fluid.

Hydrodynamic measurements and regime analysis

Experiments performed to calculate liquid velocity (v_L), the axial dispersion coefficient (ID), the N-tanks-in-series constant (N), Reynolds number (Re), bubble volume, bubble velocity, gas holdup, circulation time, and mixing time were carried out using the procedures and analytical methods described by Babcock et al. (2002). The operating range of sparger gas flow to both the NHTR and the ENHTR was 2 to 25 L min^{-1}, with 12 L min^{-1} as the typical operating value. WEF (1996) and Babcock et al. (2002) describe how liquid velocity, v_l (m s^{-1}), and axial dispersion coefficient ID (m^2 s^{-1}) can be calculated using the residence time distribution from an injected salt tracer.

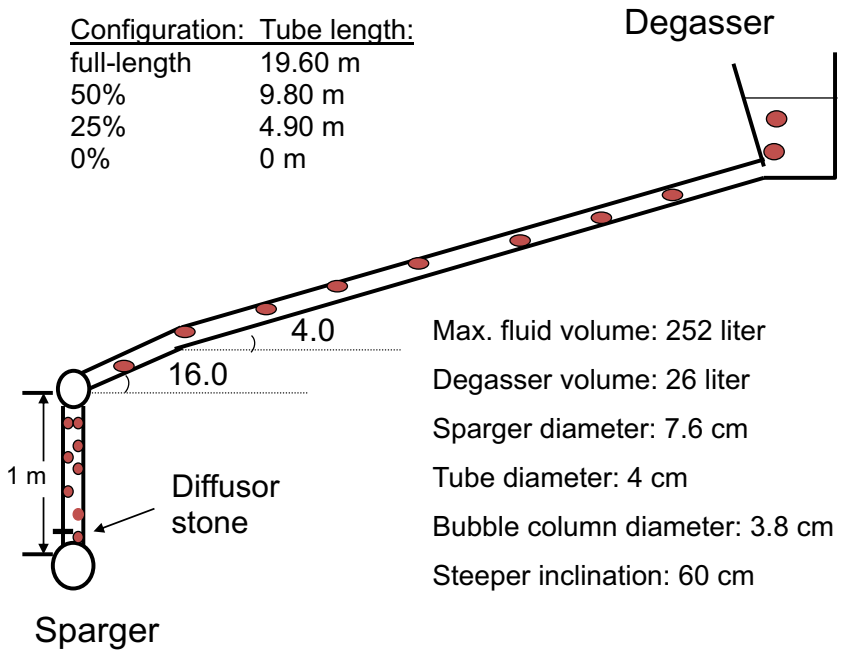

Fig. 1 Schematic diagram of the ENHTR

Mass transfer of oxygen and carbon dioxide

The mass transfer of oxygen and carbon dioxide were evaluated in the NHTR and ENHTR designs using the American Society of Civil Engineers (ASCE) 2–91 protocol of oxygen mass transfer (ASCE 1992) modified as described in Babcock et al. (2002). Mass transfer was analyzed by determining the overall volumetric mass transfer coefficients at 20 °C for oxygen ($K_La_O^{20}$) and carbon dioxide ($K_La_C^{20}$) in tap water (28 °C). Prior to each experiment, the water level in the reactor was standardized by adjusting the airflow to the rate selected for the experiment; then, the water volume was adjusted to a fixed level in the degasser. Mass transfer measurements were made with the photobioreactors at full, half, one-quarter, and zero tube lengths in separate experiments to investigate where the mass transfer occurs in the reactors.

As described in Babcock et al. (2002). the water in the reactor was supersaturated with O_2, using pure oxygen with the sparging air supply turned off, after which, the pure oxygen sparging was stopped, air sparging commenced, and dynamic mass transfer (deoxygenation) was measured. For oxygen saturation to be greater than 200 % within the degasser of the ENHTR, 5–10 min of oxygen sparging was required. This is a decrease of 30–50 % compared to the NHTR, which took 10–15 min. The two-parameter nonlinear regression technique was used to estimate K_La with the following model:

$$C = C_\infty^* - \left(C_\infty^* - C_0\right)e^{-K_La^* t} \quad (1)$$

where C is the DO (mg L^{-1}) at time t, C_∞^* is the saturation DO (mg L^{-1}), C_0 is the DO at time 0, t is time (h), and K_La is the overall gas-liquid mass transfer coefficient (h^{-1}), with all values corrected to 20 °C. Values were corrected to 20 °C using $(K_La)_T=(K_La)_{20}\,\theta^{T-20}$, where θ is 1.024 and T is liquid temperature (ASCE 1992). In the previous work, CO_2 mass transfer coefficients were calculated rather than being measured (Babcock et al. 2002). In the present work, $K_La_C^{20}$ was directly measured using a procedure analogous to that used for O_2 (supersaturation with CO_2 followed by measurement of carbon stripping). Pure CO_2 was sparged (with the air off) to reduce the reactor pH from 7.0 to 4.7, then, the CO_2 was curtailed and air sparging commenced. During CO_2 stripping, the pH was monitored. Using the measured alkalinity of the water and carbonate equilibrium speciation equations, the total concentration of inorganic carbon species was calculated at each time step while the pH increased from 5.0 to 6.5, forming the de-carbonation curve for fitting with Eq. 1. We do not know of other reports using this technique to measure K_La for CO_2. While this procedure is a logical extension of the ASCE oxygen method and our results were repeatable, it is not a standard method and may have unknown limitations that might make it inaccurate.

Mass transfer rates in the photobioreactors can be compared by calculating the standard deoxygenation rate at 20 °C, N_O^{20}, and the standard carbonation rate, N_C^{20}, calculated as the product of K_La^{20}, the saturation concentration (C_∞^*), and the volume of water in the reactor (V_{water}) as shown in Eq. 2. The C_∞^* was assumed to be constant (10 mg L^{-1}) for deoxygenation (based upon a dimensionless Henry's constant of 31 and a mole fraction of 0.20 in air). The value of $C^*{}_\infty$ for carbonation is a controllable variable based upon the amount of pure CO_2 added to the sparging air based upon a dimensionless Henry's constant of 1.1. If the mole fraction were

0.012, C_∞^* would be 20 mg L^{-1} for carbonation, and if the mole fraction were 0.021, then C_∞^* would be 35 mg L^{-1}.

$$N_i^{20} = K_L a^{20} \times C_\infty^* \times V_{water} \quad (2)$$

Using results from the hydrodynamics and mass transfer experiments, a regime analysis was performed. A regime analysis consists of a comparison of characteristic times calculated for the different mechanisms in a reactor, allowing the rate-limiting step to be determined (Babcock et al. 2002). The characteristic times were determined for mass transfer of O_2 and CO_2, bubble saturation, bubble exhaustion, and gas phase retention. For mass transfer of O_2 and CO_2, the characteristic time is the inverse of $K_L a$. The values for bubble saturation and bubble exhaustion are equal to the dimensionless Henry's constant divided by $K_L a$. The characteristic time for gas phase retention is the bubble velocity times the tube length. The circulation and mixing times were directly measured.

Results

Hydrodynamics

Hydrodynamic experiments in the NHTR and the ENHTR were performed in full-length reactors (19.6 m) at nominal gas flowrates between approximately 6 and 23 L min^{-1} (0.027–0.104 L L^{-1} min^{-1} for NHTR and 0.024–0.091 L L^{-1} min^{-1} for ENHTR). Table 1 compares the design parameters including the Reynolds number (*Re*), liquid velocity (v_l), dispersion coefficient (ID), and number of CFSTRs in series (*N*), which were determined from salt tracer tests for both reactor designs. Liquid velocity remained the same in the original NHTR and ENHTR at approximately 0.07 m s^{-1} (Babcock et al. 2002). There was greater axial mixing in the ENHTR than within the NHTR as seen in the larger dispersion coefficient due to the completely mixed bubble columns. This led to a decrease in the value of N-tanks-in-series constant from 40–70 to 24–39; however, this is still within the range of a plug flow reactor. The ENHTR can be thought of as a plug flow reactor connected on each end to a completely mixed reactor (when the degasser sparger is operated).

Table 1 Comparison of hydrodynamic parameters for the NHTR and the ENHTR. Range is for lowest and highest nominal air sparging rates of 6 and 23 L min^{-1}

Parameter	NHTR	ENHTR
Re (–)	2100–3400	2400–3200
v_l (m s^{-1})	0.06–0.08	0.06–0.08
ID (m^2 s^{-1})	0.008–0.020	0.021–0.027
N (number of CFSTRs in series)	40–70	24–39

Figure 2 shows the mixing time experiment results for the ENHTR that is estimated to be 15 min. This is equal to approximately three circulation times (5 min each). In the NHTR, the mixing time was previously reported as 60 min, which equaled ten circulation times (Babcock et al. 2002). Thus, the ENHTR modifications made the mixing time four times faster than the NHTR.

Mass transfer of oxygen and carbon dioxide

Figure 3 shows the measured overall mass transfer coefficients at 20 °C, $K_L a_O^{20}$ and $K_L a_C^{20}$, versus the nominal sparging rate for the NHTR and the ENHTR. The results indicate the ENHTR achieved $K_L a_O^{20}$ values between 100 and 175 % greater than the NHTR, which was the primary goal of the enhancements. The values of $K_L a_C^{20}$ also increased, but much less so, from 0 to 34 %. The smaller increases in measured $K_L a_C^{20}$ values were not necessarily expected, but were verified in repeat trials. The data indicate that $K_L a$ increases with greater sparging rate for both gases and reactors. However, while the NHTR values begin to level off as sparging rate increases, the ENHTR values do not, and therefore, might benefit significantly from even higher sparging rates than those tested herein. A better comparison of overall mass transfer is possible using N_i^{20} because the effect of reactor volume is included.

Figure 4 shows the values of the calculated overall mass transfer rates at 20 °C, N_O^{20} and N_C^{20}, versus the nominal sparging rate for the NHTR and the ENHTR assuming a C_∞^* value of 20 mg L^{-1} for CO_2 so that the curves would fit on the same plot. The value of C_∞^* for tap water and air is fixed (10 mg L^{-1}), but it is a variable for CO_2 enriched air. The results indicate the ENHTR had N_O^{20} values between 128 and 213 % greater than the NHTR. The values of N_C^{20} increased between 3 and 51 % and these percentages are not affected by the choice of C_∞^*. The improvements are most pronounced at the highest sparging rates (18 to 23 L min^{-1}).

Figure 5 shows a comparison of gas holdup in the NHTR and the ENHTR and shows that the total amount of gas in the ENHTR increases only slightly. We conclude that the improvements in mass transfer rates are due to the addition of fine bubbles in the VBCs that greatly increase the surface area available for mass transfer.

The standard deoxygenation rate, N_O^{20}, was measured in different reactor tube length configurations (zero, one-quarter, half, full). The N_O^{20} values for reactor length zero represent the bubble columns plus degasser. The results in Fig. 6 show that N_O^{20} tends to increase with increasing sparging rates. Results also suggest limitations based on reactor length. Oxygen stripping rates were almost equal in the full-length reactor configuration and the 50 % reactor configuration (90–95 %), with the highest stripping rate in the full-length reactor. N_O^{20} was consistently lower in the 25 and 0 % configurations. There is no significant benefit in reactors

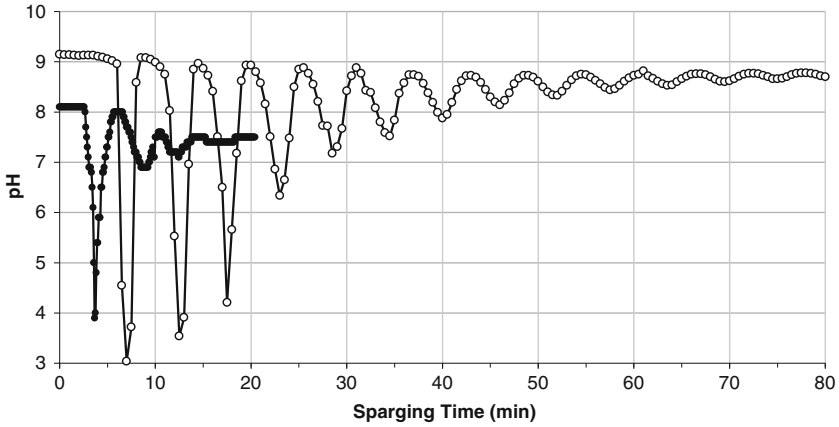

Fig. 2 Mixing times in the NHTR (*white circle*) and ENHTR (*black circle*) at a nominal gas sparging rate of 12 L min^{-1}

at the full-length configuration since 85–90 % of the mass transfer in the near-horizontal tubes occurs in the lower half.

Figure 7 compares percentage of mass transfer of oxygen and carbon dioxide, N_O^{20} and N_C^{20}, respectively, in different components of the ENHTR at a nominal sparging rate of 12 L min^{-1}: bubble columns, horizontal tubes, unaerated degasser, and aerated degasser (extra air=12 L min^{-1}). The largest portion of O_2 and CO_2 mass transfer occurred in the bubble columns and horizontal tubes. It can be observed that deoxygenation and decarbonation both increase with additional aeration in the degasser, which can improve oxygen stripping, but would be detrimental to carbonation. Also, this might be less cost effective than elongating the bubble columns, especially considering that the additional degasser aeration would double the total flowrate for air sparging (12 L min^{-1} in the bubble columns and also in the degasser).

One can calculate theoretical CO_2 consumption and O_2 generation rates for a given areal biomass productivity and these theoretical rates can be equated to necessary mass transfer rates in a photobioreactor. For a given productivity, the CO_2 requirement was calculated as the product of productivity and an assumed requirement of 1.83 g CO_2 per g biomass produced (Weissman et al. 1988) and the horizontal plane surface area of the reactor tubes. The O_2 generation rate was calculated the same way by assuming 1 mol of O_2 produced per mol of CO_2 consumed. These theoretical rates are plotted as lines in Fig. 8 which also shows the mass transfer rate ranges calculated from the measured K_La_O in Fig. 4 for NHTR and ENHTR (for nominal gas sparging rates between approximately 10 and 23 L min^{-1}). For the NHTR, the range of possible O_2 mass transfer rate is approximately 175–225 mg min^{-1}. It can be observed that the largest theoretical productivity in the NHTR is approximately 1.6 g m^{-2} h^{-1} with respect to O_2 stripping and that the necessary CO_2 mass transfer rate to achieve this productivity would be approximately 315 mg min^{-1} (following the arrows to the CO_2 line). Using the K_La_C value of 5.5 h^{-1} in Fig. 3 for a nominal sparging rate

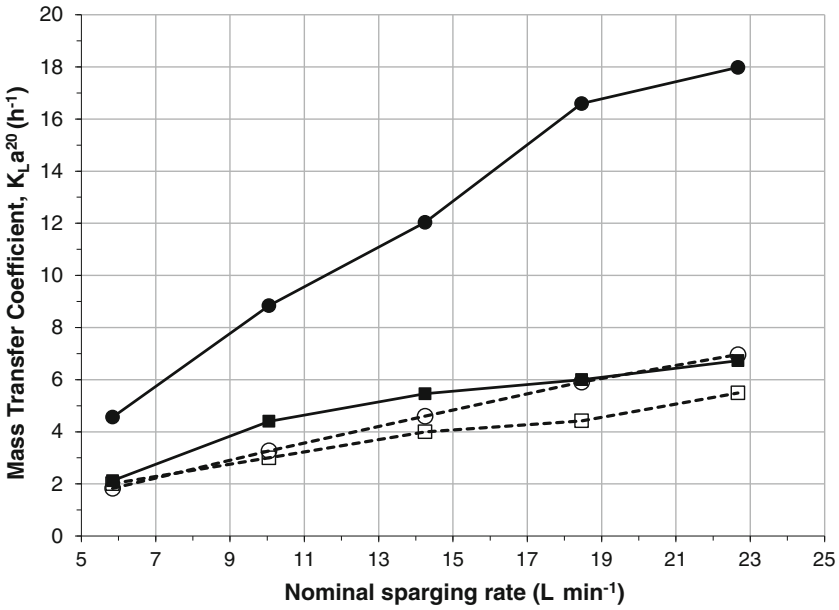

Fig. 3 Overall mass transfer coefficients in NHTR for oxygen (*black square*) and carbon dioxide (*white square*) and in ENHTR for oxygen (*black circle*) and carbon dioxide (*white circle*) as a function of nominal gas sparging rate

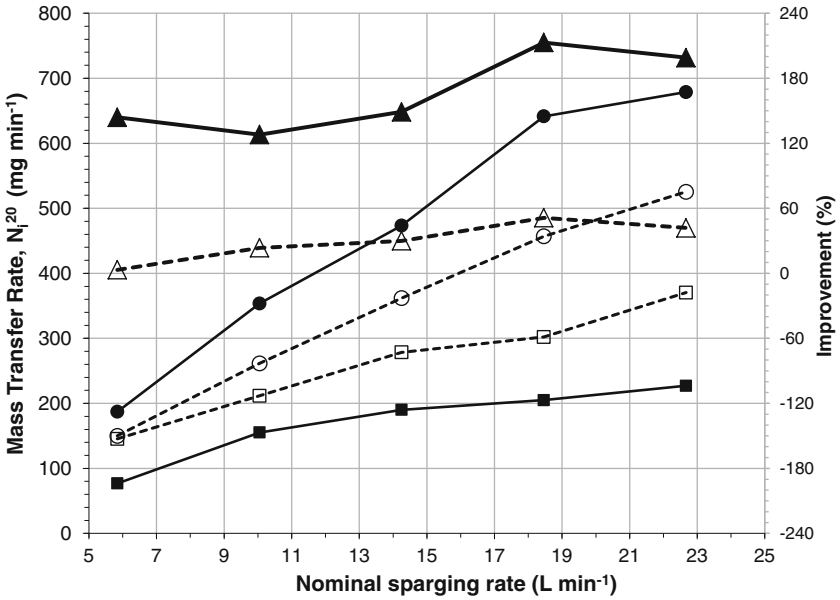

Fig. 4 Mass transfer rates in NHTR for oxygen (*black square*) and carbon dioxide (*white square*) and in ENHTR for oxygen (*black circle*) and carbon dioxide (*white circle*) and percentage increase in the ENHTR compared to the NHTR for oxygen (*black triangle*) and carbon dioxide (*increment*) as a function of nominal gas sparging rate (assumes 1.2 % CO_2 in sparger gas enriched from 0.04 % in air)

of 22.7 L min^{-1}, the required value of C_∞^* is calculated from Eq. 2 (15.6 mg L^{-1}) and using the Henry's coefficient of 1.1, the amount of CO_2 required in the enriched sparging gas is calculated as 0.92 % (compared to 0.04 % in standard air). This agrees fairly well with our previous experience cultivating *Arthrospira* in which we achieved a maximum of 1.5 g m^{-2} h^{-1} at densities up to 7.5 g L^{-1} in the NHTR (Radway et al. 1999). For the ENHTR, the working range of mass transfer increased to approximately 350–680 mg min^{-1}. It can be observed that the largest theoretical productivity in the ENHTR is approximately 4.75 g m^{-2} h^{-1} and the required CO_2 mass transfer rate to achieve this productivity would be approximately 940 mg min^{-1}. Using K_La_C and Henry's law, the calculated amount of CO_2 required in the sparging gas would be 1.9 % to achieve this increased productivity.

Table 2 shows a comparison of the calculated characteristic times for a regime analysis of the NHTR and the ENHTR. Comparison of the time constants for mass transfer between liquid and gas phases with gas phase retention time shows that the ENHTR is an improvement over the NHTR (smaller mass transfer times and larger gas phase retention); however, there is not enough time for complete mass transfer to occur in the tubes (Table 2). Comparison of the time constants for bubble saturation with oxygen and those for gas phase retention shows that the bubbles will not become saturated and therefore oxygen will still accumulate in the culture media in the ENHTR, even though the constants are improved compared to the NHTR. Comparison of the constants for carbon dioxide exhaustion and gas phase retention give rise to a similar conclusion that the bubbles in the ENHTR

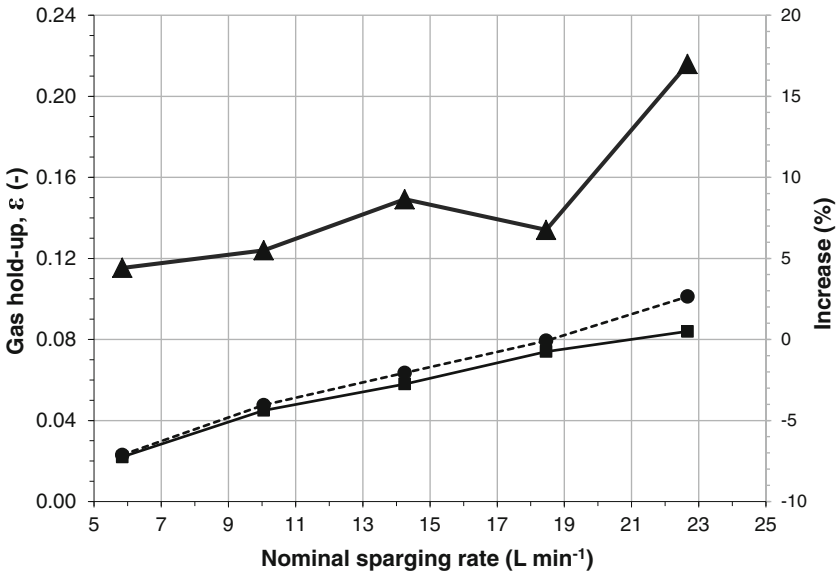

Fig. 5 Gas holdup in NHTR (*black square*) and ENHTR (*black circle*) and percentage increase in the ENHTR compared to the NHTR (*black triangle*) as a function of nominal gas sparging rate

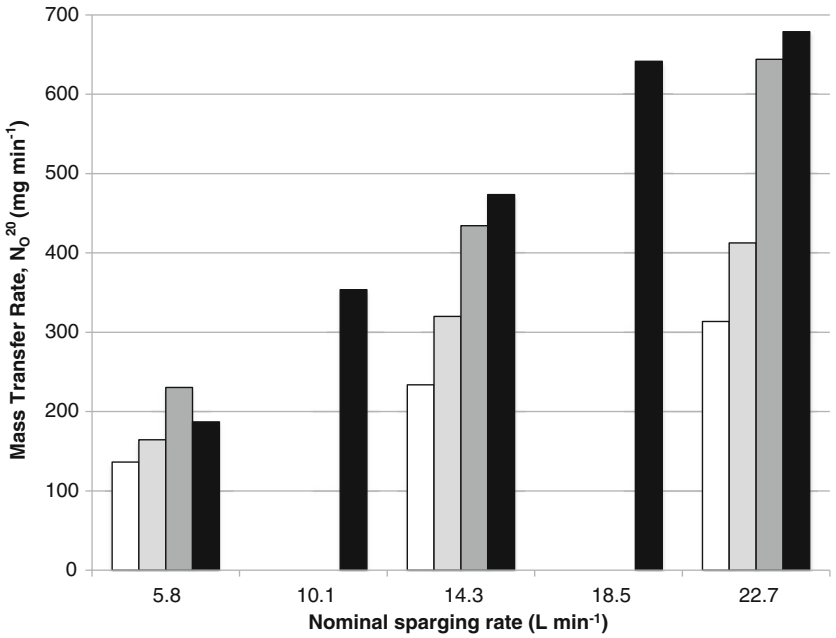

Fig. 6 Oxygen mass transfer rates in the ENHTR bubble columns (*white square*) and different sections of the horizontal tubes ENHTR: 25 % tube length (▫), 50 % tube length (▪), and 100 % full length tubes (*black square*) as a function of nominal gas sparging rate

(although better than the NHTR) will not be exhausted of carbon dioxide, which will be wasted in the degasser. Because the characteristic times for mass transfer of both gases are smaller than the mixing times, there will be gradients of these gases in both the NHTR and the ENHTR. The regime analysis indicates that mass transfer limitations have been reduced in the ENHTR relative to the NHTR; however, it is still mass-transfer limited.

Discussion

Performance based on hydrodynamics and mass transfer comparisons was assessed in the Tredici NHTR and the ENHTR photobioreactor designs. Accepted standard techniques (ASCE 1992) were used to measure mass transfer of oxygen. The possible limitations of this technique in plug-flow reactors were discussed in detail previously (Babcock et al. 2002). and the determined K_La_O values compared favorably to those published by others (Camacho Rubio et al. 1999) for a 220-L horizontal serpentine reactor (3.4 to 7.2 h^{-1}). We have used the method to evaluate K_La_O in the only slightly modified ENHTR to evaluate improvements. As described above, we attempted herein to extend this mass transfer measurement technique to directly measure K_La_C rather than simply calculating theoretical values based on diffusivities. As described in our previous work (Babcock et al. 2002). the theoretical K_La_C should be 90 % of K_La_O; however, the K_La_C values measured for the NHTR range from 60 to 95 % of the K_La_O values and the values range from 36 to 40 % in the ENHTR. If the

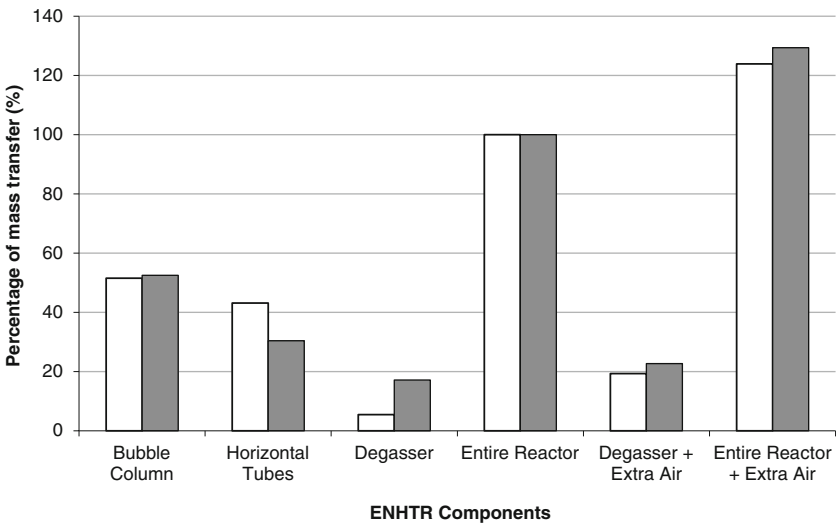

Fig. 7 Percentage of mass transfer rates of oxygen (*white square*) and carbon dioxide (*black aquare*) in segments of the ENHTR at a nominal sparging rate of 12 L min^{-1}

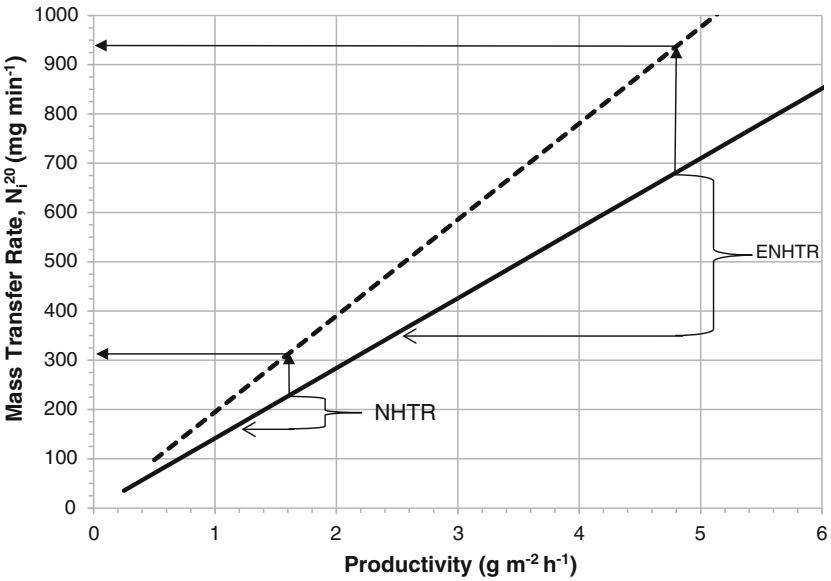

Fig. 8 Comparison of required mass transfer rates of oxygen (*solid line*) and carbon dioxide (*dotted line*) as a function of theoretical areal productivity with calculated values of oxygen mass transfer rate in the NHTR and ENHTR. *Arrows* indicate how to determine the required carbon dioxide mass transfer rate for the maximum rates of oxygen transfer in the NHTR and the ENHTR

measured values of CO_2 mass transfer coefficients are not correct and instead the K_La_C should be 90 % of K_La_O, then the required values for CO_2 gas enrichment of the sparging air would be slightly smaller than those calculated above but this would not affect the fact that the hydrodynamics and mass transfer have been improved in the ENHTR and this will result in greater areal productivity (predicted theoretical improvement of up to 200 %).

Potential further improvements to enhance mass transfer of O_2 include additional sparger aeration, additional degasser aeration, making the near-horizontal reactor tubes longer, making the bubble columns longer, and increasing the diameter of all the reactor tubes. The current results can be used to make extrapolations for these various potential enhancements as follows. Examination of Fig. 3 indicates that K_La_O may increase with additional sparger air and level off at about 20 h^{-1} which is about a 10 % further increase in oxygen stripping and possibly a similar percent increase in productivity. Additional degasser aeration would lead to additional O_2 stripping; however, the increase is small relative to the amount of additional sparger air required and there is a simultaneous increase in CO_2 stripping from the media. Any CO_2 not dissolved into the media from the large bubbles that reach the degasser is lost to the atmosphere. For this reason, it could be beneficial to lengthen the VBCs and/or the reactor tubes to enhance the O_2 mass transfer rate. Increasing the length of the bubble columns from 1 to 2 m could double the K_La values in that section of the reactor (where 50 % of the mass transfer occurs) leading to 25 % larger limiting N_O^{20} values and a theoretical productivity of 5.9 g m^{-2} h^{-1}. This improvement could be extrapolated further for any length of VBCs. Another option is to increase the horizontal reactor tube lengths to 40 m, in which case, the K_La's might not increase at all (because very little mass transfer occurs past the first 10 m). This would mean a doubling of O_2 mass transfer rate and a doubling of required CO_2 mass transfer rate, leading to no increase in productivity. Similarly, shortening the reactor horizontal tube length to 10 m also leads to no theoretical increase in productivity. The effects of increasing the tube diameter are more difficult to predict.

Table 2 Characteristic times for the NHTR and the ENHTR in tap water at a nominal gas flow rate of 22.7 L min^{-1}

Phenomenon	Characteristic time (s)	
	NHTR	ENHTR
Mass transfer of oxygen	565	200
Mass transfer of carbon dioxide	656	517
Bubble saturation with oxygen	16,580	6207
Bubble exhaustion of carbon dioxide	721	569
Gas phase retention	48	55
Circulation time	360	300
Mixing time	3600	900

In conclusion, modifications to the original Tredici NHTR photobioreactor resulted in significant hydraulic and mass transfer improvements in the enhanced version. Addition of fine-bubble aerated vertical bubble columns to the diffuser end of the reactor improved the mass transfer rates and would theoretically enhance productivity. Based on a regime analysis, the ENHTR will still experience gradients of oxygen and carbon dioxide in the reactor and will still be mass transfer limited. In this study, we directly measured both oxygen and carbon dioxide mass transfer coefficients, separately. After calculating mass transfer rates and comparing to carbon

dioxide nutrient input requirements and oxygen stripping requirements, we found that productivity could be tripled by adding a 1-m length bubble column to the sparger end of the NHTR using typical nominal sparging rates. In addition, further significant improvements in productivity are not expected from increasing the length of the near horizontal tubes from 20 to 40 m, but significant additional improvements are possible by increasing the vertical bubble column length to 2 m or longer.

Acknowledgments This work was supported in part by US National Science Foundation Grant No. EEC-9731725. This research was made possible through a collaboration with Dr. Mario R Tredici at the University of Florence who designed the original near horizontal tubular photobioreactor. Helpful comments and suggestions were made by Dr. Joseph C Weissman.

References

ASCE (1992) Measurement of oxygen transfer in clean water, ANSI/ASCE standard 2–91, 2nd edn. American Society of Civil Engineers, New York, pp 1–41

Babcock RW Jr, Malda J, Radway JC (2002) Hydrodynamics and mass transfer in a tubular airlift photobioreactor. J Appl Phycol 14:169–184

Béchet Q, Chambonnière P, Shilton A, Guizard G, Guieysse B (2015) Algal productivity modeling: a step toward accurate assessments of full-scale algal cultivation. Biotechnol Bioeng 112:987–996

Camacho Rubio FC, Acien Fernandez FG, Sanchez Perez JA, Garcia Camocho F, Molina Grima E (1999) Prediction of dissolved oxygen and carbon dioxide concentration profiles in tubular photobioreactor for microalgal culture. Biotechnol Bioeng 62:71–86

Chini Zittelli G, Lavista F, Bastianini A, Rodolfi L, Vincenzini M, Tredici MR (1999) Production of eicosapentaenoic acid by *Nannochloropsis* sp. cultures in outdoor tubular photobioreactors. J Biotechnol 70:299–312

Del Campo JA, García González M, Guerrero MG (2007) Outdoor cultivation of microalgae for carotenoid production: current state and perspectives. Appl Microbiol Biotechnol 74:1163–1174

García Malea MC, Del Río E, Casas López JL, Acién Fernández FG, Fernández Sevilla JM, Rivas J, Guerrero MG, Molina Grima E (2006) Comparative analysis of the outdoor culture of *Haematococcus pluvialis* in tubular and bubble column photobioreactors. J Biotechnol 123:329–342

Kang Z, Kim BH, Ramanan R, Choi JE, Yang JW, Oh HM, Kim HS (2015) A cost analysis of microalgal biomass and biodiesel production in open raceways treating municipal wastewater and under optimum light wavelength. J Microbiol Biotechnol 25:109–118

Radway JC, Yoza BA, Benemann JR, Babcock RW Jr, Weissman JC, Chini Zitelli G, Tredici MR (1999) Evaluation of a near-horizontal tubular photobioreactor in Hawaii. Proceedings 8th Intl. Conf. On Applied Algology, Motecatini Terme, Italy

Vonshak A (1997) Outdoor mass production of *Spirulina*: the basic concept. In: Vonshak A (ed) *Spirulina platensis* (*Arthrospira*): physiology, cell-biology and biotechnology. Taylor and Francis, Bristol, pp 79–99

Wang S, Chen J, Li Z, Wang Y, Fu B, Han X, Zheng L (2015) Cultivation of the benthic microalga *Prorocentrum lima* for the production of diarrhetic shellfish poisoning toxins in a vertical flat photobioreactor. Bioresour Technol 179:243–248

WEF (1996) Wastewater disinfection, manual of practice FD10. Water Environment Federation, Alexandria, pp 61–99

Weissman JC, Goebel RP, Benemann JR (1988) Photobioreactor design: mixing, carbon utilization, and oxygen accumulation. Biotechnol Bioeng 31:336–344